Regulation of fibroblast growth factor-23 expression in osteoblasts by calciprotein particles

Calciprotein particles regulate fibroblast growth factor-23 expression in osteoblasts

OPEN

Ken-ichi Akiyama[1,2], Yutaka Miura[1], Hirosaka Hayashi[1], Asuka Sakata[3], Yoshitaka Matsumura[4], Masaki Kojima[4], Ken Tsuchiya[2], Kosaku Nitta[2], Kazuhiro Shiizaki[1], Hiroshi Kurosu[1] and Makoto Kuro-o[1,5,6]

[1]Division of Anti-aging Medicine, Center for Molecular Medicine, Jichi Medical University, Tochigi, Japan; [2]Department of Medicine, Kidney Center, Tokyo Women's Medical University, Tokyo, Japan; [3]Department of Pediatrics, Nara Medical University, Nara, Japan; [4]School of Life Sciences, Tokyo University of Pharmacy and Life Sciences, Tokyo, Japan; [5]Charles and Jane Pak Center for Mineral Metabolism and Clinical Research, Department of Internal Medicine, University of Texas Southwestern Medical Center, Dallas, Texas, USA; and [6]Japan Agency for Medical Research and Development, Japan Core Research for Evolution Science and Technology, Tokyo, Japan

Fibroblast growth factor-23 (FGF23) is a hormone indispensable for maintaining phosphate homeostasis. In response to phosphate intake, FGF23 is secreted from osteocytes/osteoblasts and acts on the kidney to increase urinary phosphate excretion. However, the mechanism by which these cells sense phosphate intake remains elusive. Calciprotein particles are nanoparticles of calcium-phosphate precipitates bound to serum protein fetuin-A and are generated spontaneously in solution containing calcium, phosphate, and fetuin-A to be dispersed as colloids. In cultured osteoblastic cells, increase in either calcium or phosphate concentration in the medium induced FGF23 expression, which was dependent on calciprotein particle formation. When transition of calcium-phosphate precipitates from the amorphous phase to the crystalline phase was blocked by bisphosphonate, the calciprotein particle size was reduced and FGF23 expression was augmented, suggesting that small calciprotein particles containing amorphous calcium-phosphate precipitates function as a more potent FGF23 inducer than larger calciprotein particles containing crystalline calcium-phosphate precipitates. In mice, bolus phosphate administration by oral gavage transiently increased circulating calciprotein particle levels followed by a modest increase in FGF23 expression and serum FGF23 levels. However, continuous dietary phosphate load induced robust and persistent increase in circulating calciprotein particles and FGF23 levels. We confirmed by *in vivo* imaging that calciprotein particles injected intravenously extravasated into the bone marrow and were deposited on the inner surface of the bone, indicating that these particles have direct access to osteoblasts. Thus, we propose that osteoblasts induce FGF23 expression and secretion when they sense an increase in extracellular calciprotein particles following phosphate ingestion.

Correspondence: *Makoto Kuro-o, Division of Anti-aging Medicine, Center for Molecular Medicine, Jichi Medical University, 3311-1 Yakushiji, Shimotsuke, Tochigi 329-0498, Japan. E-mail: mkuroo@jichi.ac.jp*

Received 14 March 2019; revised 24 September 2019; accepted 10 October 2019; published online 9 November 2019

Kidney International (2019) ■, ■–■; https://doi.org/10.1016/j.kint.2019.10.019

KEYWORDS: amorphous calcium-phosphate; crystalline calcium-phosphate; fetuin-A; osteoblasts

Translational Statement

Calciprotein particles are colloidal nanoparticles of calcium-phosphate dispersed in the blood. Calciprotein particles are increased in patients with chronic kidney disease and are regarded as pathological agents that induce inflammatory responses and vascular calcification. On the other hand, circulating levels of a bone-derived phosphaturic hormone fibroblast growth factor-23 are also increased with chronic kidney disease progression and are associated with mineral bone disorder. In this study, we show that calciprotein particles function as a physiological agent that delivers calcium-phosphate to the bone and induces fibroblast growth factor-23 expression in osteoblasts. The measurement of blood calciprotein particles levels is expected to be useful not only for a better understanding on how fibroblast growth factor-23 production/secretion is regulated but also for risk evaluation of chronic kidney disease–mineral bone disorder.

Phosphorus homeostasis at the organismal level is maintained by balancing phosphate intake and excretion. Specifically, the amount of phosphate excreted into urine is regulated so as to become equal to the amount of phosphate absorbed from the digestive tract.[1] The amount of urinary phosphate excretion is primarily regulated by the endocrine axis consisting of fibroblast growth factor-23 (FGF23) and its obligate coreceptor klotho. FGF23 is a hormone secreted from osteoblasts and osteocytes in response to phosphate intake. FGF23 binds to the binary complex of FGF receptor and klotho expressed in renal tubules and suppresses phosphate reabsorption, thereby promoting urinary phosphate excretion.[2] However, it is not clear how osteocytes/

osteoblasts sense phosphate intake to induce expression and secretion of FGF23.

A possible mechanism is that osteoblasts/osteocytes secrete FGF23 when they sense postprandial increase in the blood phosphate level through a putative "phosphate-sensing receptor." This hypothesis is analogous to the fact that parathyroid cells secrete parathyroid hormone (PTH) when they sense decrease in the blood calcium level through the calcium-sensing receptor.[3] However, several lines of evidence argue against this hypothesis. First, serum FGF23 levels were correlated not only with serum phosphate but also with calcium levels.[4] Second, increase in serum phosphate failed to raise serum FGF23 when the serum calcium level was low[5] and vice versa. Namely, in the presence of hypophosphatemia, FGF23 was not increased in response to increase in serum calcium.[4] These observations indicate that both serum calcium and phosphate concentration must be above a certain level to induce FGF23 secretion.

Calciprotein particles (CPP) are colloidal nanoparticles composed of serum protein fetuin-A laden with calcium-phosphate precipitates (CaPis) and dispersed in the blood.[6,7] We recently established a method for quantification of CPPs in the blood and found that plasma CPP levels were correlated with serum FGF23 and phosphate levels.[8] Thus, we hypothesize that it is not phosphate or calcium *per se* but CPPs that may induce FGF23 secretion and/or production in osteoblasts/osteocytes. The purpose of this study is to test this hypothesis.

RESULTS

CPP formation is associated with FGF23 induction

To determine whether increase in the extracellular calcium and phosphate can directly induce FGF23 expression in osteoblasts, we cultured rat osteoblastic cells (UMR-106), increased calcium and phosphate concentration in the medium, and measured cellular FGF23 mRNA levels by quantitative reverse transcriptase polymerase chain reaction (qPCR). FGF23 expression was increased not only with increase in phosphate but also with increase in calcium (Figure 1a). We measured CPP levels in the medium by the gel filtration method[8] and observed a linear correlation between the CPP and FGF23 mRNA levels (Figure 1b). However, when formation of CaPis was inhibited by adding citrate to the medium, both CPP and FGF23 mRNA levels were decreased (Figure 1c and d), whereas mRNA levels encoded by other genes, including cyclophilin and cytochrome P450 family 24, were not decreased (data not shown). These results are consistent with the hypothesis that formation of CPPs in the medium is necessary for osteoblastic cells to induce FGF23 expression.

Synthesized CPPs induce FGF23 expression

Next, we tested whether CPPs could increase FGF23 expression without increasing the calcium and phosphate concentration in the medium. We added synthesized CPPs to the medium of UMR-106 cells and observed a dose-dependent increase in FGF23 expression (Figure 2a). The FGF23 mRNA levels were significantly increased within 4 hours after addition of synthesized CPPs (Figure 2b), followed by increase in the FGF23 protein levels in the conditioned medium (Figure 2c). Although to a significantly lesser extent than the CPP treatment, the vehicle treatment also induced FGF23 over time (Figure 2b and c), which may reflect the effect of 1,25-dihydroxyvitamin D_3 added to the medium. We confirmed that addition of synthesized CPPs never increased but rather reduced the levels of phosphate, calcium, and calcium phosphate product in the medium before FGF23 expression was induced (Figure 2d–f). We also confirmed that the CPP levels in the medium stayed constant during the experimental period (Figure 2g). Hence, we concluded that persistent increase in the extracellular CPPs, but not increase in the phosphate or calcium concentration, is necessary and sufficient for osteoblastic cells to induce FGF23 expression.

Physical property of CPPs affect their ability to induce FGF23 expression

Amorphous CaPis undergo spontaneous transition into the thermodynamically stable crystalline phase over time.[9] Because bisphosphonate interferes with the amorphous-to-crystalline phase transition of CaPis,[10] we speculated that bisphosphonate might inhibit growth of crystalline CaPis and thus formation of CPPs, thereby attenuating the effect of increase in the extracellular calcium and phosphate concentration on FGF23 induction in osteoblasts. Contrary to our prediction, addition of alendronate to the high calcium (3 mmol/l [mM]), high phosphate (5 mM) medium augmented FGF23 expression (Figure 3a). These unexpected results led us to hypothesize that CPPs generated in the presence or absence of alendronate could be different in quality, which might have affected the ability of CPPs to induce FGF23 expression. To test this hypothesis, we performed small angle X-ray scattering analysis and characterized physical properties of CPPs generated in the high-phosphate, high-calcium medium in the presence and absence of alendronate. Because CPPs can be dissolved by chelating calcium in the medium with ethylenediamine tetraacetic acid (EDTA),[8] we extracted the X-ray scattering profile of CPPs by taking the difference before and after addition of EDTA (Figure 3b and c). In the absence of alendronate, we identified CPPs with a hydrostatic diameter of approximately 35 nm or over. By contrast, these CPPs disappeared in the presence of alendronate. Instead, smaller CPPs with a diameter of around 9.2 nm were detected, which appeared as flat particles with platelike shapes (Figure 3d). Because the size of a single fetuin-A molecule is ~7.1 nm in diameter,[11] these small particles are considered to be CPPs composed of a single fetuin-A molecule that adsorbs amorphous CaPis. In fact, the size of these particles is comparable with that of calciprotein monomers, described previously.[11] Calciprotein monomers represent fetuin-A monomers laden with Posner clusters, or $Ca_9(PO_4)_6$, which are around 0.9 nm in diameter and deemed as precursors of amorphous CaPis.[11] These observations imply that the

FLA 5.6.0 DTD ■ KINT1848_proof ■ 26 November 2019 ■ 4:42 pm ■ ce

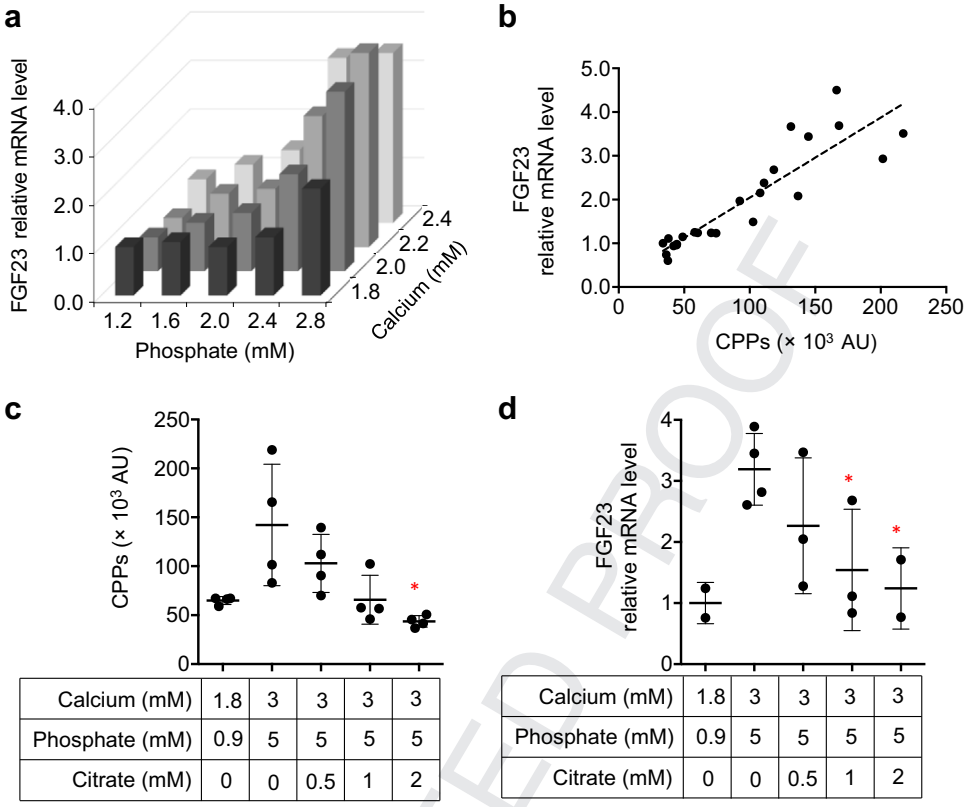

Figure 1 | Induction of fibroblast growth factor-23 (FGF23) expression in cultured osteoblastic cells is associated with calciprotein particle (CPP) formation in the medium. (**a**) Induction of FGF23 expression in UMR-106 osteoblastic cells by increasing the extracellular phosphate and calcium concentration. The FGF23 mRNA levels were quantified by quantitative reverse transcriptase polymerase chain reaction 24 hours after changing the calcium and phosphate concentration in the medium as indicated. Each bar shows the average of duplicates. (**b**) A linear correlation between FGF23 mRNA levels and CPP levels in the conditioned medium. $R^2 = 0.804$, $P < 0.0001$. (**c**) Inhibition of CPP formation by citrate. UMR-106 cells were incubated in the medium containing different concentrations of calcium, phosphate, and citrate as indicated. Twenty-four hours later, CPP levels in the conditioned medium were determined. Citrate lowered CPP levels in the medium in a dose-dependent manner. $P < 0.013$ by analysis of variance, $n = 4$ for each column. *$P < 0.05$ versus calcium/phosphate/citrate = 3/5/0 mmol/l (mM) by t test. (**d**) Inhibition of CPP formation by citrate-attenuated FGF23 expression induced by increasing extracellular calcium and phosphate concentration. Citrate lowered FGF23 mRNA levels in a dose-dependent manner. *$P < 0.05$ versus calcium/phosphate/citrate = 3/5/0 mM by t test, $n = 2 \sim 4$ for each column. AU, arbitrary unit(s). Q12

9.2-nm CPPs containing amorphous CaPis can induce FGF23 expression more robustly than the >35-nm CPPs containing crystalline CaPis. For simplicity, we designate CPPs as any colloidal particles of CaPis bound to fetuin-A, regardless of whether the fetuin-A is a monomer or multimers, although significant difference may exist between CPPs and calciprotein monomers in terms of function and clearance.

Bolus phosphate ingestion increases blood CPP and FGF23 levels

Provided that osteoblasts produce/secrete FGF23 in response to phosphate intake by sensing CPPs in the blood, the following findings should be observed. First, blood CPP levels should be increased after dietary phosphate intake, followed by increase in FGF23 mRNA levels in the bone and FGF23 protein levels in the blood. Second, blood CPPs should extravasate in the bone marrow and have direct access to osteoblasts and/or osteocytes. To verify these predictions, we first administered phosphate in mice (6-week-old male animals, C57BL/6) by oral gavage and determined how FGF23 mRNA levels in the bone and blood levels of phosphate, calcium, CPPs, PTH, 1,25-dihydroxyvitamin D_3, and FGF23 would be changed over time. Serum FGF23 levels were measured in 2 distinct assays—c-terminal FGF23 (cFGF23) enzyme-linked immunosorbent assay (ELISA) and intact FGF23 (iFGF23) ELISA.[12] In the cFGF23 ELISA, both the capture and detection antibodies recognize the C-terminal portion of FGF23. On the other hand, the iFGF23 ELISA consists of the capture antibody that binds to the N-terminal portion and the detection antibody that binds to the C-terminal portion of FGF23. Because FGF23 is inactivated by proteolytic cleavage to produce the N-terminal and C-terminal fragments,[13] iFGF23 represents the active fraction of FGF23, whereas cFGF23 represents the total amount of secreted FGF23 protein including both active and inactive FGF23.

We observed increase in serum CPP, phosphate, and PTH levels and decrease in serum calcium levels within 2 hours, which restored to the basal levels within 4 to 6 hours

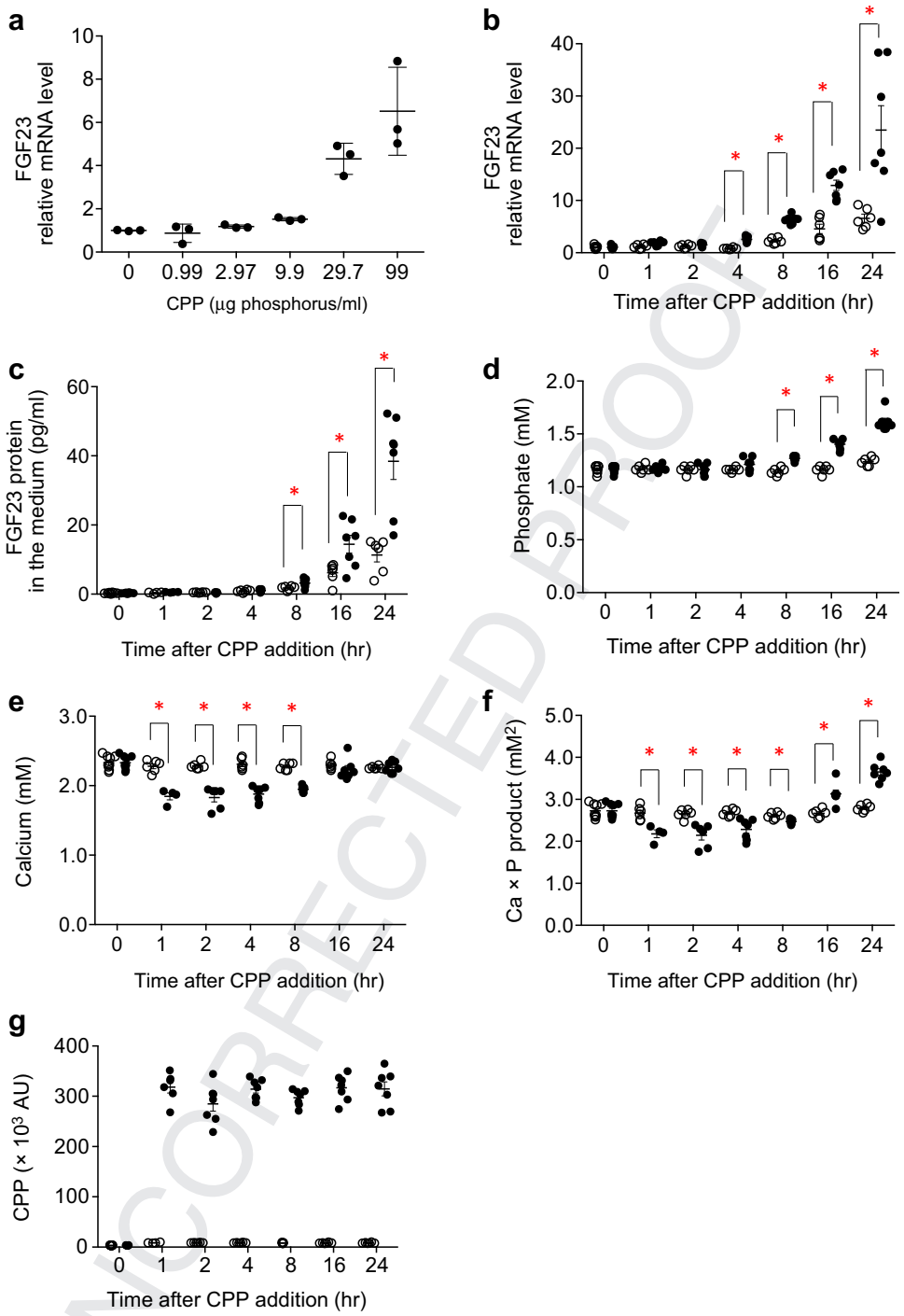

Figure 2 | Calciprotein particles (CPPs) induce fibroblast growth factor-23 (FGF23) expression in cultured osteoblastic cells. (**a**) Synthesized CPPs induce FGF23 expression in a dose-dependent manner. $P < 0.0001$ by analysis of variance, $n = 3$ for each column. CPPs were synthesized and prepared as described in the Methods. The indicated doses of synthesized CPPs were added to the medium. Twenty-four hours later, the cellular FGF23 mRNA levels were measured by quantitative reverse transcriptase polymerase chain reaction. (**b**) A time course of FGF23 induction by synthesized CPPs. The cellular FGF23 mRNA levels were quantified by quantitative reverse transcriptase polymerase chain reaction at the indicated time points after addition of 29.7 μg phosphorus/ml of CPPs (solid columns) or vehicle (open columns) to the medium. *$P < 0.05$ versus vehicle by t test, $n = 4 \sim 8$ for each column. (**c**) A time course of CPP-induced increase in FGF23 secretion into the medium. FGF23 protein levels in the conditioned medium were quantified by enzyme-linked immunosorbent assay for C-terminal FGF23 at the indicated time points after addition of 29.7 μg phosphorus/ml of CPPs (solid columns) or vehicle (open columns) to the medium. The conditioned medium was concentrated before being subjected to the enzyme-linked immunosorbent assay. *$P < 0.05$ versus vehicle by t test, $n = 4 \sim 8$ for each column. Levels of (**d**) phosphate, (**e**) calcium, (**f**) calcium phosphate product, and (**g**) CPPs in the conditioned medium at the indicated time points after addition of 29.7 μg phosphorus/ml of CPPs (solid columns) or vehicle (open columns) to the medium. *$P < 0.05$ versus vehicle by t test, $n = 4 \sim 9$ for each column. AU, arbitrary unit(s); M, mol/l.

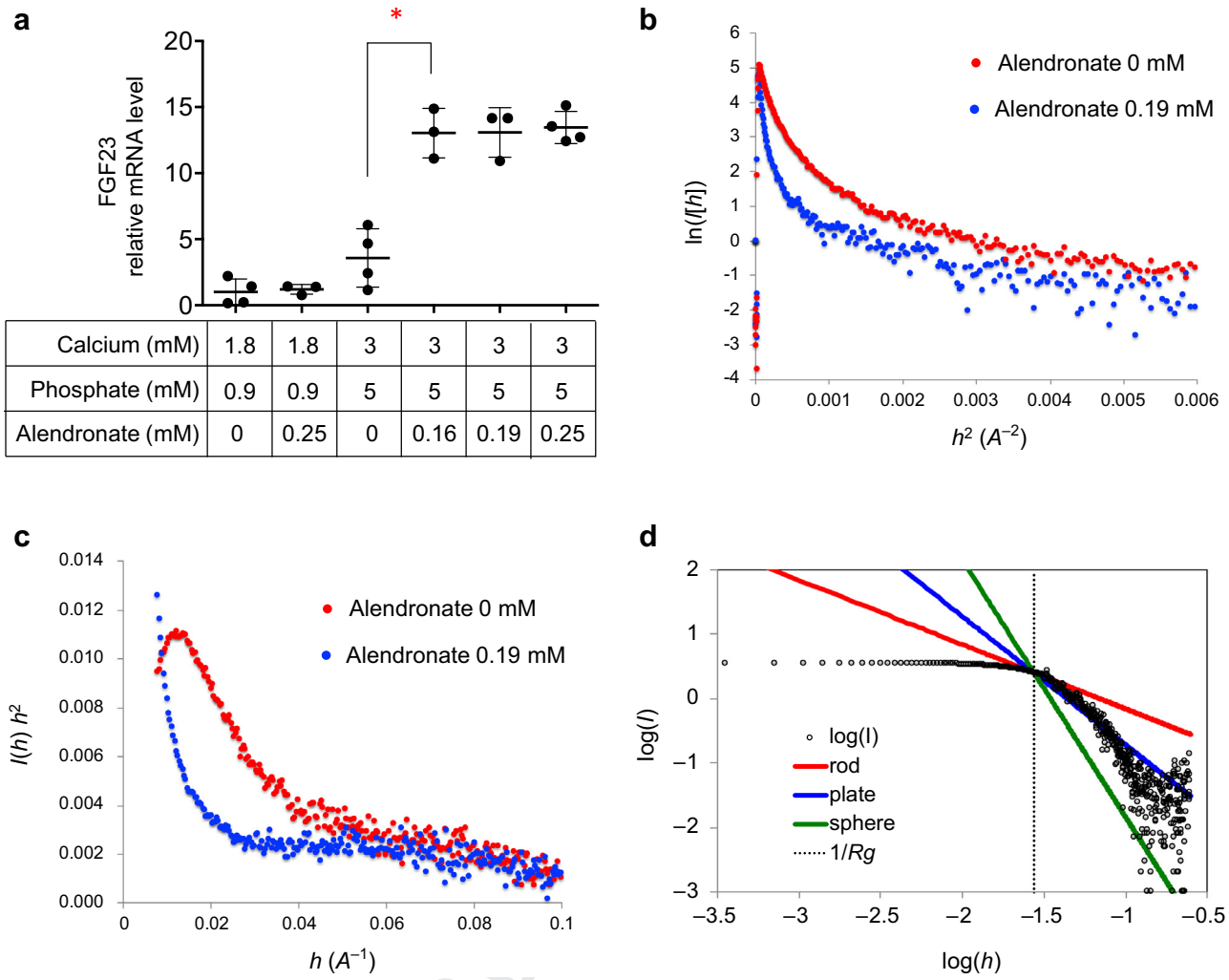

Calcium (mM)	1.8	1.8	3	3	3	3
Phosphate (mM)	0.9	0.9	5	5	5	5
Alendronate (mM)	0	0.25	0	0.16	0.19	0.25

Figure 3 | Physical properties of calciprotein particles (CPPs) affect their ability to induce fibroblast growth factor-23 (FGF23) expression in cultured osteoblasts. (**a**) Inhibition of the amorphous-to-crystal phase transition of calcium-phosphate precipitates by alendronate potentiates the ability of CPPs to induce FGF23 expression. UMR-106 cells were cultured in the medium containing the indicated concentration of calcium, phosphate, and alendronate for 24 hours and then analyzed by quantitative reverse transcriptase polymerase chain reaction to quantify FGF23 mRNA levels. *$P < 0.05$ versus calcium/phosphate/alendronate = 3/5/0 mmol/l (mM) by t test, $n = 3 \sim 4$ for each column. Analysis of the small angle x-ray scattering curves by (**b**) Guinier plots and (**c**) Kratky plots of the conditioned medium from UMR-106 cells incubated with calcium/phosphate/alendronate = 3/5/0 mM (red) and 3/5/0.19 mM (blue) for 20 hours. The radius of gyration *Rg* of CPPs in the absence and presence of alendronate was estimated as 136.5 and 36 Å, respectively, which correspond to 17.6 nm and 4.6 nm in hydrostatic radius *Rh* provided that CPPs are spheres with uniform density ($Rh = 1.29\ Rg$). (**d**) The double logarithm plot of CPPs that informs the shape of particles. Fitted lines were approximated as cylindrical (red), flat (blue), and spherical (green) particles.[26]

(Figure 4a–d). In contrast, FGF23 mRNA levels and serum FGF23 levels were not increased significantly until 4 hours after the phosphate ingestion (Figure 4e–g), indicating that increase in plasma CPP levels preceded the increase in FGF23. The similar time course was observed in the serum 1,25-dihydroxyvitamin D_3 levels (Figure 4h). Although 1,25-dihydroxyvitamin D_3 has the ability to induce FGF23 expression in osteoblasts,[14] the increase in 1,25-dihydroxyvitamin D_3 cannot explain the increase in serum FGF23 levels, because the FGF23 mRNA levels showed a decreasing trend when the 1,25-dihydroxyvitamin D_3 levels were increased. These observations suggest that CPPs, but not 1,25-dihydroxyvitamin D_3, may primarily contribute to FGF23 induction on bolus phosphate ingestion.

Blood CPPs extravasate in the bone marrow

Blood CPP and phosphate levels started increasing within 2 hours after the phosphate gavage and returned to the basal level within 4 hours, indicating that CPPs and phosphates were cleared from the blood. Because CPPs are nanoparticles, it is implausible that such large particles are filtrated through glomerulus and excreted into urine like phosphate is. However, it is possible that CPPs may exit from blood vessels through sinusoids, which are capillary beds composed of endothelial cells with large fenestrations. Sinusoids exist in

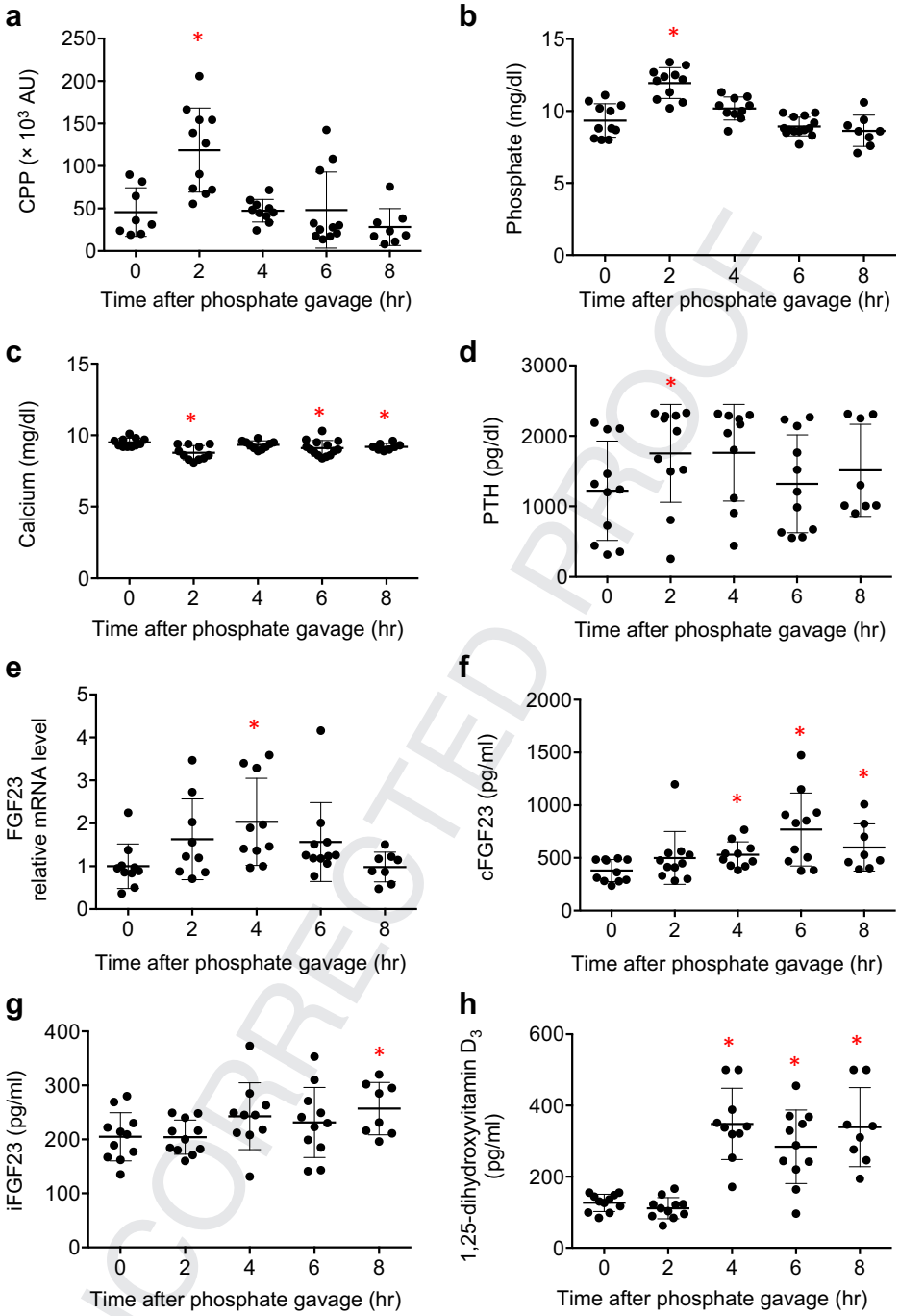

Figure 4 | Bolus phosphate ingestion increases blood calciprotein particles (CPPs) and fibroblast growth factor-23 (FGF23) levels in mice. The time course of changes in (**a**) plasma CPPs, (**b**) serum phosphate, (**c**) serum calcium, (**d**) serum parathyroid hormone (PTH), (**e**) cellular FGF23 mRNA, (**f**) serum C-terminal FGF23 (cFGF23), (**g**) serum intact FGF23 (iFGF23), and (**h**) serum 1,25-dihydroxyvitamin D_3 after administered with phosphate by oral gavage. *$P < 0.05$ versus 0 hours (before phosphate administration) by t test, $n = 8 \sim 11$ for each column. AU, arbitrary unit(s).

the liver and the bone marrow. To determine whether CPPs could extravasate in the liver and the bone marrow, we administered synthesized CPPs fluorescently labeled with fluorescein isothiocyanate (FITC)–conjugated alendronate into mice by tail vein injection and performed *in vivo* imaging. We confirmed that injected CPPs were phagocytosed by Kupffer cells in the liver as previously reported[15] (Figure 5a– c, Supplementary Movies S1 and S2). By *in vivo* imaging of the calvaria, we found that injected CPPs were deposited on the bone surface facing the marrow cavity where osteoblasts reside (Figure 5d and e, Supplementary Movies S3–S5). We conclude that blood CPPs can exit from blood vessels in the bone and reach osteoblasts directly.

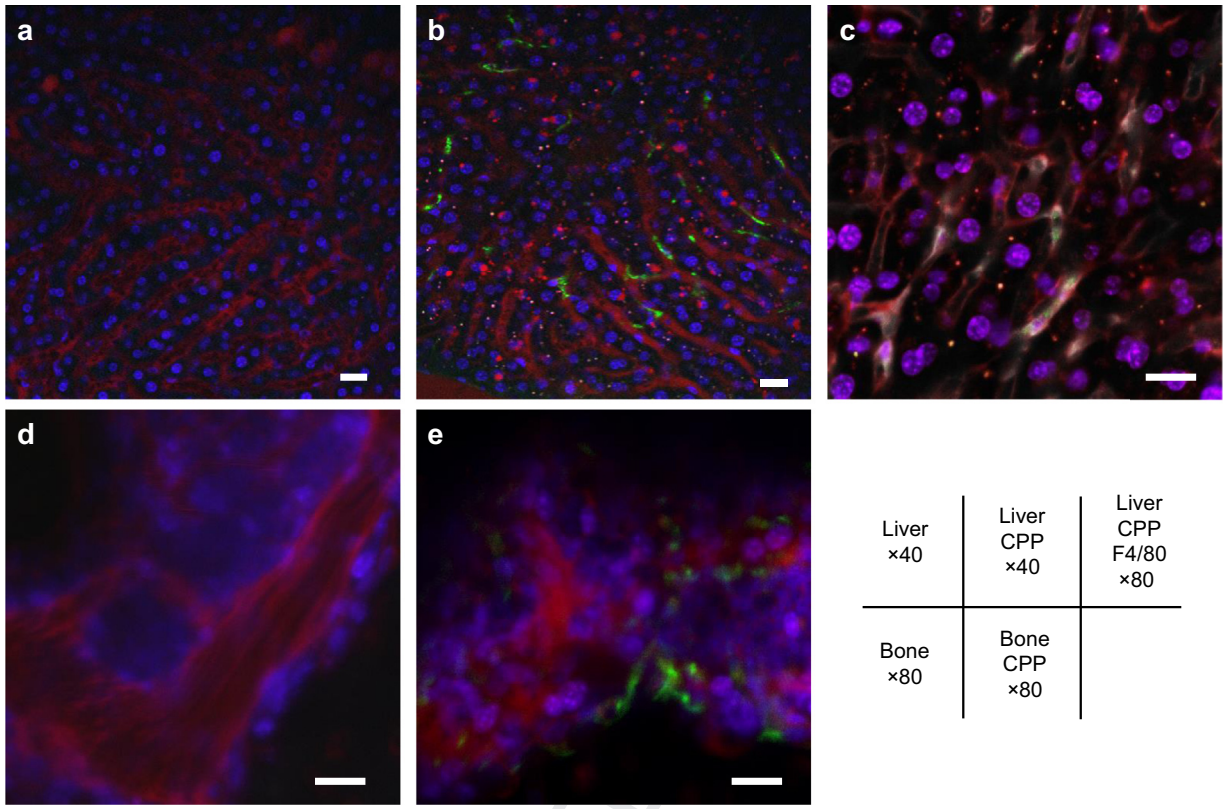

Figure 5 | Blood calciprotein particles (CPPs) extravasate in the liver and bone marrow in mice. *In vivo* imaging of the liver (**a**) before and (**b**) after i.v. injection of CPPs labeled with fluorescein isothiocyanate (green). (**c**) As in **b**, except that an antibody against F4/80 was injected to label Kupffer cells (white). Signals from CPPs (green) overlap with Kupffer cells (white). *In vivo* imaging of the calvaria (**d**) before and (**e**) after i.v. injection of fluorescein isothiocyanate–labeled CPPs. Bars = 20 μm. Blood vessels and cell nuclei were visualized with 70 kD dextran labeled with rhodamine (red) and Hoechst (blue). To optimize viewing of this image, please see the online version of this article at www.kidney-international.org. Q13

print & web 4C/FPO

Dietary phosphate load increases blood CPP and FGF23 levels

Because increase in dietary phosphate intake was reported to elevate serum FGF23 levels,[4] we asked whether plasma CPP levels would be increased after dietary phosphate load. We placed mice (8-week-old male, C57BL/6) on a high phosphate diet containing 2.0% inorganic phosphate for 2 days and observed that these mice had significantly higher plasma CPP levels than did mice placed on a regular diet containing 0.35% inorganic phosphate (Figure 6a). We also found that the dietary phosphate load caused significant increase in serum FGF23 (both cFGF23 and iFGF23), phosphate, PTH, and 1,25-dihydroxyvitamin D_3 levels and marginal decrease in calcium levels in the blood (Figure 6b–g). FGF23 mRNA levels in the bone were also significantly increased by feeding the high phosphate diet (Figure 6h). Thus, unlike bolus phosphate ingestion, continuous dietary phosphate load causes persistent increase in plasma CPPs and robust increase in serum FGF23.

DISCUSSION

Plasma CPP levels were increased after phosphate ingestion (Figures 4a and 6a). Because FGF23 functions as a phosphaturic hormone as well as a counterregulatory hormone for 1,25-dihydroxyvitamin D_3,[2] FGF23 should exert negative impact on CPP formation through lowering phosphate concentration in the extracellular fluid by inducing phosphaturia and through inhibiting calcium absorption in the digestive tract by lowering circulating a1,25-dihydroxyvitamin D_3 levels. Thus, the ability of CPPs to induce FGF23 may be required for a negative feedback loop to prevent increase in the circulating CPP level, which is associated with vascular calcification, aortic stiffness, and inflammation in patients with chronic kidney disease (CKD).[16,17]

Koppert *et al.*[18] recently reported that synthesized secondary CPPs were endocytosed by Kupffer cells by intravital 2-photon imaging, which was consistent with the finding of our *in vivo* imaging. However, they did not describe deposition of CPP to the bone. This may be simply because they did not look at the bone or because the CPPs used in their studies were different from the CPPs used in our present study. They used high-density secondary CPPs precipitated by centrifugation at 20,000*g* for 20 minutes. In contrast, we used CPPs that passed through a gel-filtration spin column with the size-exclusion limit at 40 kDa,[8] which contained not only high-density CPPs equivalent to the secondary CPPs they used but also low-density CPPs that were not precipitated by the centrifugation.[8] It remains to be determined whether the low-density CPPs may be

FLA 5.6.0 DTD ■ KINT1848_proof ■ 26 November 2019 ■ 4:42 pm ■ ce

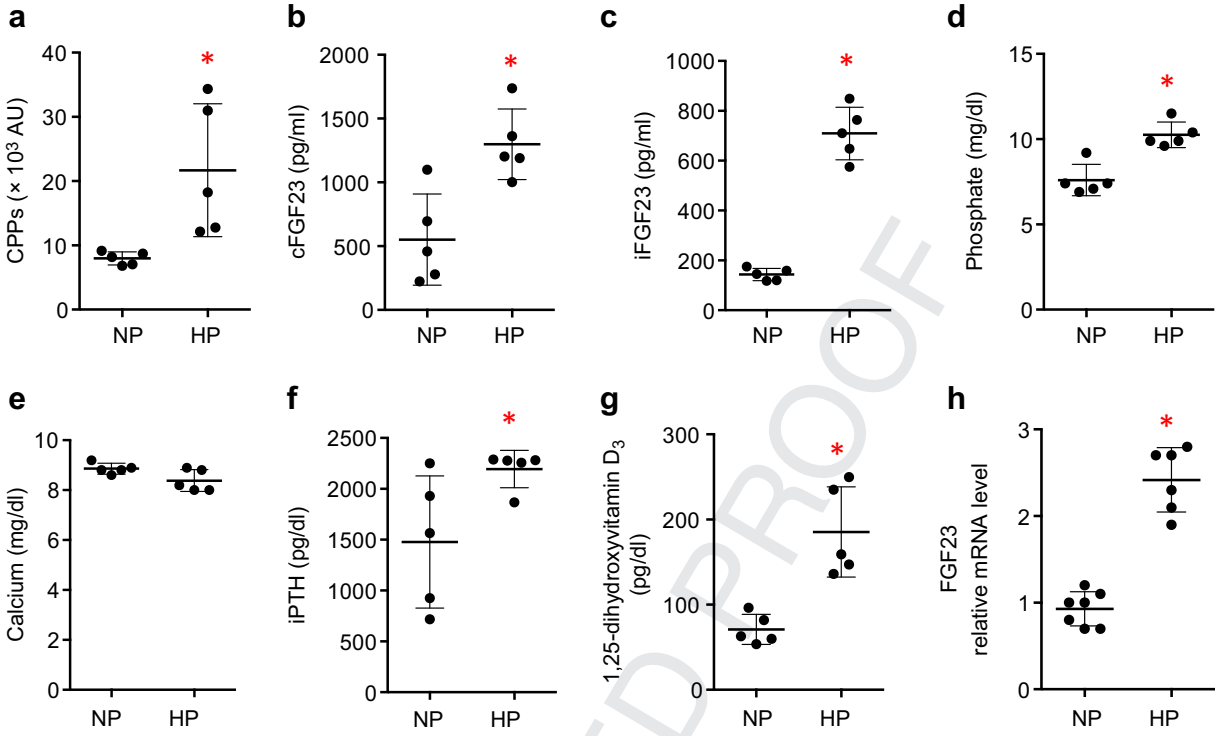

Figure 6 | Dietary phosphate load increases blood calciprotein particles (CPPs) and fibroblast growth factor-23 (FGF23) levels in mice. Mice were placed on diet containing 0.35% (NP) or 2.0% (HP) inorganic phosphate for 2 days and then used for measurement of (**a**) plasma CPPs, (**b**) serum C-terminal FGF23 (cFGF23), (**c**) serum intact FGF23 (iFGF23), (**d**) serum phosphate, (**e**) serum calcium, (**f**) serum parathyroid hormone (iPTH), (**g**) serum 1,25-dihydroxyvitamin D_3, and (**h**) cellular FGF23 mRNA levels. *$P < 0.05$ versus NP by *t* test, $n = 5$ for each column. AU, arbitrary units.

efficiently deposited to the bone when compared with high-density secondary CPPs.

In the present mouse study, bolus phosphate ingestion increased phosphate and CPPs but reciprocally decreased calcium within 2 hours, which was accompanied by increase in PTH. These changes were restored to the basal levels within 4 to 6 hours (Figure 4a–d). In contrast to these quick responses, significant increase in bone FGF23 mRNA and serum FGF23 levels did not become evident until 4 hours after the phosphate ingestion when serum phosphate levels had already started decreasing (Figure 4e–g). This slow response of FGF23 indicates that the phosphaturic activity of FGF23 did not contribute to the restoration of serum phosphate levels after the bolus phosphate ingestion. This is also applicable to humans.[19] In addition, the ratio of cFGF23 to iFGF23 (c/iFGF23 ratio), which represents the activity of proteolytic inactivation of FGF23, was increased followed by the increase in the FGF23 mRNA level (Supplementary Figure S1A), suggesting an attempt to attenuate the FGF23 activity. These observations suggest that phosphaturic activity of PTH may be primarily responsible for the quick restoration of the serum phosphate level after bolus phosphate ingestion. Hence, in this context, physiological significance of the delayed increase in FGF23 is unclear.

In contrast to bolus phosphate ingestion, continuous dietary phosphate load by placing mice on high phosphate diet for 2 days caused persistent and robust increase in CPP and FGF23 levels (Figure 4a–c). This is consistent with the results of *in vitro* experiment showing that induction of FGF23 secretion in cultured osteoblastic cells required incubation with CPPs for 8 hours or longer (Figure 2c). Additionally, unlike bolus phosphate ingestion, continuous dietary phosphate load significantly decreased the c/iFGF23 ratio (Supplementary Figure S1B), suggesting an attempt to limit proteolytic inactivation of FGF23. Reduction of c/iFGF23 ratio is observed under the condition where phosphaturic activity of FGF23 is required to maintain phosphate homeostasis like CKD.[12] In fact, injection of a neutralizing Q6 antibody against FGF23 to CKD mice raised serum phosphate levels before PTH started decreasing,[20] indicating that it is not PTH but FGF23 that had primarily contributed to maintaining phosphate homeostasis in CKD. It appears that PTH and FGF23 are primarily responsible for maintaining phosphate homeostasis in response to acute and chronic phosphate load, respectively. In contrast, increase in c/iFGF23 ratio is observed under the condition where FGF23 is produced more than is necessary. For example, administration of bisphosphonate into mice fed high phosphate diet elevated serum levels of cFGF23, but not iFGF23, resulting in increase in the c/iFGF23 ratio (Supplementary Figure S2). This is consistent with the *in vitro* finding that treatment with bisphosphonate

FLA 5.6.0 DTD ■ KINT1848_proof ■ 26 November 2019 ■ 4:42 pm ■ ce

increased FGF23 expression in osteoblastic cells cultured in high phosphate medium (Figure 3a).

The mechanism by which CPPs induce FGF23 and inflammatory responses including upregulation of the osteopontin[21] and dentin matrix protein-1[22] (Supplementary Figure S3) in osteoblasts remains to be determined. Hori *et al.*[23] reported that induction of FGF23 expression in UMR-106 cells by increasing phosphate in the medium was dependent on production of reactive oxygen species (ROS) and that increase in FGF23 expression induced by hydrogen peroxide was blocked by a mitogen-activated protein kinase inhibitor PD98059. Because CPPs were reported to stimulate ROS production in cultured macrophages[24] and vascular smooth muscle cells,[25] it is plausible that induction of FGF23 expression in osteoblasts by CPPs may be also mediated through ROS production followed by activation of the mitogen-activated protein kinase pathway. Therefore, we tested whether increase in FGF23 expression by CPPs might be also blocked by PD98059. However, the effect of PD98059 on CPP-induced increase in FGF23 expression was modest (Supplementary Figure S4), indicating that factors other than ROS might contribute to increase in FGF23 expression induced by CPPs.

METHODS

Animals

For the bolus phosphate ingestion experiment, mice (C57BL/6, 6-week-old males) were starved overnight, administered with 10 μl/g body weight of 0.5 M phosphate buffer (mixture of 0.5 M NaH_2PO_4 and 0.5 M Na_2HPO_4, pH 7.4) by oral gavage, and killed at the indicated time points to harvest the blood and calvaria. For the continuous dietary phosphate load experiment, mice (C57BL/6, 8-week-old male) were placed on either a regular diet containing 0.35% inorganic phosphate or a high phosphate diet containing 2.0% inorganic phosphate for 2 days and then sacrificed to harvest the blood and calvaria. For bisphosphonate treatment, we placed C57BL6 male mice at 12 weeks of age on the regular diet or the high phosphate diet for 10 days. Mice placed on high phosphate diet were treated with either alendronate (10 mg/kg, s.c. injection) or vehicle (saline) every other day. All animal experiments were approved by the institutional animal care and use committee from Jichi Medical University.

Cell culture

A rat osteoblastic cell line UMR-106 was purchased from ATCC (CRL-1661; Manassas, VA) and cultured in growth medium consisting of Dulbecco's Modified Eagle's Medium ([DMEM]; Nacalai Tesque, Kyoto, Japan) supplemented with 10% fetal bovine serum (Biological Industries, Beit Haemek, Israel). When the cells reached near-confluency on 12-well plates (Corning, Corning, NY), the growth medium was replaced with the experimental medium (1 ml/well) consisting of DMEM containing 40 mg/ml of bovine serum albumin (Sigma-Aldrich, St. Louis, MO), 0.5 mg/ml bovine fetuin-A (Sigma-Aldrich), and 1 nM of 1,25-dihydroxyvitamin D_3 (Sigma-Aldrich). Twenty-four hours later, the medium was replaced with the experimental medium (1 ml/well) containing indicated calcium and phosphate concentration and further incubated for indicated time periods.

Preparation of the high phosphate high calcium medium

The concentration of calcium and phosphate in DMEM is 1.8 mM and 0.9 mM, respectively. The experimental medium containing higher calcium and phosphate concentration was prepared as follows: First, calcium-free and phosphate-free DMEM (In) were supplemented with 40 mg/ml of bovine serum albumin, 0.5 mg/ml bovine fetuin-A, 10 mM *N*-2-hydroxyethylpiperazine-*N*′-2-ethanesulfonic acid (pH 7.4), and 1 nM of 1,25-dihydroxyvitamin D_3. Second, 1 M phosphate buffer was added to the calcium-free DMEM to bring the phosphate concentration to 2-fold higher than the desired final concentration. Likewise, 1 M $CaCl_2$ was added to the phosphate-free DMEM to bring the calcium concentration to 2-fold higher than the desired final concentration. Lastly, the calcium-free DMEM and the phosphate-free DMEM were mixed in the volume ratio of 1:1.

Quantification of FGF23 mRNA levels

UMR-106 cells on the plate were washed with phosphate-buffered saline and then homogenized with RNAiso Plus (TaKaRa Bio Inc., Shiga, Japan). Mouse calvaria was frozen in liquid nitrogen and then crushed using Cryo-Press (MICROTEC Co., Ltd., Chiba, Japan) before being homogenized with RNAiso Plus. The lysate was transferred to a microcentrifuge tube and extracted with chloroform. RNA in the aqueous phase was precipitated with isopropanol, washed with 75% ethanol, and dissolved in RNase-free water. Reverse transcription of RNA (0.4 μg) was carried out using ReverTra Ace qPCR RT Master Mix with gDNA Remover (FSQ-301; Toyobo Co., Ltd., Osaka, Japan) according to the manufacturer's protocol. qPCR reactions contained 20 ng of cDNA, 410 nM of each primer, and 6 μl of SYBR Green PCR Master mix (THUNDERBIRD SYBR qPCR Mix QPS-201, Toyobo) in a total volume of 12 μl. The PCR reaction (95 °C for 1 minute followed by 45 cycles of 95 °C for 10 seconds, 60 °C for 40 seconds) was performed on a LightCycler 480 system (Roche Diagnostics, Rotkreuz, Switzerland). Relative mRNA levels were calculated by the comparative threshold cycle method using cyclophilin as an internal control. The nucleotide sequence of the primers were GCCAGTGGACGCTAGAGAAC (forward) and TGATGCTTCGGTGACAGGTA (reverse) for FGF23, GATCGATAGTGCCGAGAAGC (forward) and TGAAACTCGTGGCT CTGATG (reverse) for osteopontin, TCCAGTGAAGACAGCACGTC (forward) and CATCACTGTGGTGGTCCTTG (reverse) for dentin matrix protein-1.

CPP assay

Quantification of CPPs in the cell culture medium and mouse blood was performed as previously reported.[8] Briefly, a fluorescent probe that binds to CaPi crystals (OsteoSense 680EX; PerkinElmer Inc., Waltham, MA) was added to concentrated medium or heparin plasma samples. After incubation at 25 °C for 60 minutes, the sample was applied to a gel-filtration spin column to remove unbound OsteoSense. The fluorescent intensity of the flow-through was quantified using an infrared fluorescence scanner (Odyssey CLx; LI-COR Biosciences, Lincoln, NE).

CPP synthesis

Phosphate-free DMEM and calcium-free DMEM were supplemented with 40 mg/ml of bovine serum albumin and 0.5 mg/ml bovine fetuin-A. CPPs were synthesized by mixing 20 ml of the phosphate-free DMEM with its calcium concentration adjusted at 6 mM and the same volume of the calcium-free DMEM with its phosphate concentration adjusted at 10 mM to make the final concentration of

FLA 5.6.0 DTD ■ KINT1848_proof ■ 26 November 2019 ■ 4:42 pm ■ ce

calcium and phosphate at 3 mM and 5 mM, respectively. The mixture was incubated at 37 °C for 16 hours and then centrifuged at 16,000*g* for 2 hours. After removal of the supernatant, the precipitated CPPs were suspended with 0.4 ml of the experimental medium (1.8 mM calcium, 0.9 mM phosphate) and applied to UMR-106 cells grown on 12-well plates at indicated doses. CPPs generated under these experimental conditions contained 1.66 μg of calcium and 0.99 μg of phosphorus per microliter as determined by inductively coupled plasma mass spectrometry. Briefly, 100 μl of the CPP preparation was diluted with 10 ml of concentrated nitric acid (98%) and digested using Titan MPS microwave (PerkinElmer) according to the manufacturer's protocol for digestion of milk. Phosphorus (P^{31}) and calcium (Ca^{44}) content in the digested samples were measured using inductively coupled plasma mass spectrometry Nexion 2000 (PerkinElmer) by the kinetic energy discrimination mode with helium and argon as the collision gas and reaction gas, respectively. Calibration curves were generated using standards for calcium and phosphorus (PerkinElmer) at 0.10, 0.99, and 10.00 mg/l.

Small angle X-ray scattering

Small angle X-ray scattering analysis was performed using NANOPIX (Rigaku, The Woodlands, TX). Scattering intensities *I(h)* were obtained for each sample before and after addition of EDTA at the final concentration of 5 mM. *I(h)* is the function of momentum transfer at $h = 4\pi \sin \theta/\lambda$, where 2θ and λ indicate the scattering angle and the wavelength of X-ray (1 Å), respectively. The difference in *I(h)* before and after the EDTA treatment was defined as the scattering from CPPs. The radius of gyration R_g was estimated by double exponential Guinier analyses where 2 components were assumed. The R_g value was also estimated from the peak position of the Kratky plot with the equation as $R_g = \sqrt{3}/h$. The hydrostatic radius R_h was estimated as $R_h = \sqrt{5/3}R_g$.

Blood and medium analysis

FGF23 was measured using mouse/rat FGF23 (C-Term) ELISA (Immutopics International, San Clemente, CA) and intact FGF23 ELISA (Kinos) according to the manufacturers' protocols. For measurement of FGF23 in the conditioned medium of UMR-106 cells, the medium was concentrated using Amicon Ultra centrifugal filters (2 ml, 3K; Merck Millipore, Billerica, MA) before subjected to the ELISA. PTH was measured using an ELISA kit for mouse PTH (CEA866Mu; Cloud-Clone, Katy, TX). Calcium and phosphate were measured using Fuji Dri-Chem slides and the analyzer (Dri-Chem NX500V; Fuji Holdings, Tokyo, Japan). Active vitamin D (1,25-dihydroxyvitamin D3) was measured by radio-immunoassay.

In vivo imaging

Twenty (20) μl of 100 mg/ml rhodamin B-dextran (70 kD; Sigma-Aldrich) and 50 μl of 62.5 mg/ml Hoechst 33342 (Invitrogen, Thermo Fisher Scientific, Waltham, MA) were administered to anesthetized mice (C57BL/6, 8-week-old male) by tail vein injection for visualizing blood vessels and cell nuclei. Alendronate was conjugated with FITC and purified by high performance liquid chromatography. Purified FITC-alendronate was used to fluorescently label CPPs. CPPs synthesized as described above were incubated with FITC-alendronate (final concentration at 5 μM) for 30 minutes at room temperature and then applied to a gel-filtration spin column to remove unbound FITC-alendronate. For imaging of the bone, the skull surface was surgically exposed, and immediately after administration of FITC-labeled CPPs from external jugular vein, subjected to *in vivo* imaging. CPP signals in the bone marrow were detected by single-photon imaging. A 2-photon image of the same region was captured to visualize collagen bone by second harmonic generation signals. For imaging of the liver, the median lobe of the liver was surgically exposed, and the FITC-labeled CPPs were injected to the external jugular vein together with 50 μl of Alexafluor 647 anti-mouse F4/80 antibody (0.5 mg/ml; BioLegend, San Diego, CA) to label Kupffer cells. Liver cells and CPPs were visualized by single-photon imaging. All images were acquired by inverted 2-photon excitation microscopy (A1R-MP; Nikon, Tokyo, Japan).

DISCLOSURE

All the authors declared no competing interests.

ACKNOWLEDGMENTS

The authors thank Ms. Yuko Shimizu, Ms. Taeko Yamauchi, and Mr. Yukinari Ohsaka (Jichi Medical University) for technical assistance; Ms. Kyoko Nakamura (Jichi Medical University) for administrative assistance; and Drs. Ruri Kaneda, Toshihiro Nakano, Yoshitaka Hirano, Marina Miura, Yoshitaka Iwazu (Jichi Medical University), and Hidekazu Sugiura (Tokyo Women's Medical University) for discussion. This work was supported in part by Japan Agency for Medical Research and Development–Japan Core Research for Evolution Science and Technology Grant JP19gm0610012, Japan Agency for Medical Research and Development, Japan Society for the Promotion of Science KAKENHI Grant JP16H05302, and a grant from Bristol-Myers Squibb Foundation.

SUPPLEMENTARY MATERIAL

Figure S1. Effects of phosphate ingestion on the ratio of cFGF23 to iFGF23.
Figure S2. Differential effects of bisphosphonate on cFGF23 and iFGF23 in mice under dietary phosphate load.
Figure S3. Inflammatory responses induced by high calcium high phosphate medium in osteoblastic cells.
Figure S4. Effects of MEK inhibition on FGF23 expression induced by high calcium high phosphate medium in osteoblastic cells.
Movie S1. *In vivo* imaging of the liver before CPP injection (single-photon).
Movie S2. *In vivo* imaging of the liver after CPP injection (single-photon).
Movie S3. *In vivo* imaging of the bone marrow in calvarium before CPP injection (single-photon).
Movie S4. *In vivo* imaging of the bone marrow in calvarium before CPP injection (2-photon).
Movie S5. *In vivo* imaging of the bone marrow in calvarium after CPP injection (single-photon).
Supplementary material is linked to the online version of the paper at www.kidney-international.org.

REFERENCES

1. Schiavi SC, Kumar R. The phosphatonin pathway: new insights in phosphate homeostasis. *Kidney Int*. 2004;65:1–14.
2. Hu MC, Shiizaki K, Kuro-o M, et al. Fibroblast growth factor 23 and klotho: physiology and pathophysiology of an endocrine network of mineral metabolism. *Annu Rev Physiol*. 2013;75:503–533.
3. Brown EM, Gamba G, Riccardi D, et al. Cloning and characterization of an extracellular Ca(2+)-sensing receptor from bovine parathyroid. *Nature*. 1993;366:575–580.
4. Quinn SJ, Thomsen AR, Pang JL, et al. Interactions between calcium and phosphorus in the regulation of the production of fibroblast growth factor 23 in vivo. *Am J Physiol Endocrinol Metab*. 2013;304:E310–E320.
5. Rodriguez-Ortiz ME, Lopez I, Munoz-Castaneda JR, et al. Calcium deficiency reduces circulating levels of FGF23. *J Am Soc Nephrol*. 2012;23:1190–1197.

6. Heiss A, DuChesne A, Denecke B, et al. Structural basis of calcification inhibition by alpha 2-HS glycoprotein/fetuin-A: formation of colloidal calciprotein particles. *J Biol Chem*. 2003;278:13333–13341.
7. Kuro-o M. Klotho, phosphate and FGF-23 in ageing and disturbed mineral metabolism. *Nat Rev Nephrol*. 2013;9:650–660.
8. Miura Y, Iwazu Y, Shiizaki K, et al. Identification and quantification of plasma calciprotein particles with distinct physical properties in patients with chronic kidney disease. *Sci Rep*. 2018;8:1256.
9. Dorozhkin SV. Amorphous calcium (ortho)phosphates. *Acta Biomater*. 2010;6:4457–4475.
10. Fleisch H. Diphosphonates: history and mechanisms of action. *Metab Bone Dis Relat Res*. 1981;3:279–287.
11. Heiss A, Pipich V, Jahnen-Dechent W, et al. Fetuin-A is a mineral carrier protein: small angle neutron scattering provides new insight on fetuin-a controlled calcification inhibition. *Biophys J*. 2010;99:3986–3995.
12. Smith ER, Cai MM, McMahon LP, et al. Biological variability of plasma intact and C-terminal FGF23 measurements. *J Clin Endocrinol Metab*. 2012;97:3357–3365.
13. Shimada T, Muto T, Urakawa I, et al. Mutant FGF-23 responsible for autosomal dominant hypophosphatemic rickets is resistant to proteolytic cleavage and causes hypophosphatemia in vivo. *Endocrinology*. 2002;143:3179–3182.
14. Shimada T, Hasegawa H, Yamazaki Y, et al. FGF-23 is a potent regulator of vitamin D metabolism and phosphate homeostasis. *J Bone Miner Res*. 2004;19:429–435.
15. Herrmann M, Schafer C, Heiss A, et al. Clearance of fetuin-A–containing calciprotein particles is mediated by scavenger receptor-A. *Circ Res*. 2012;111:575–584.
16. Hamano T, Matsui I, Mikami S, et al. Fetuin-mineral complex reflects extraosseous calcification stress in CKD. *J Am Soc Nephrol*. 2010;21:1998–2007.
17. Smith ER, Ford ML, Tomlinson LA, et al. Phosphorylated fetuin-A-containing calciprotein particles are associated with aortic stiffness and a procalcific milieu in patients with pre-dialysis CKD. *Nephrol Dial Transplant*. 2012;27:1957–1966.
18. Koppert S, Buscher A, Babler A, et al. Cellular clearance and biological activity of calciprotein particles depend on their maturation state and crystallinity. *Front Immunol*. 2018;9:1991.
19. Nishida Y, Taketani Y, Yamanaka-Okumura H, et al. Acute effect of oral phosphate loading on serum fibroblast growth factor 23 levels in healthy men. *Kidney Int*. 2006;70:2141–2147.
20. Hasegawa H, Nagano N, Urakawa I, et al. Direct evidence for a causative role of FGF23 in the abnormal renal phosphate handling and vitamin D metabolism in rats with early-stage chronic kidney disease. *Kidney Int*. 2010;78:975–980.
21. Lund SA, Giachelli CM, Scatena M. The role of osteopontin in inflammatory processes. *J Cell Commun Signal*. 2009;3:311–322.
22. Dussold C, Gerber C, White S, et al. DMP1 prevents osteocyte alterations, FGF23 elevation and left ventricular hypertrophy in mice with chronic kidney disease. *Bone Res*. 2019;7:12.
23. Hori M, Kinoshita Y, Taguchi M, et al. Phosphate enhances Fgf23 expression through reactive oxygen species in UMR-106 cells. *J Bone Miner Metab*. 2016;34:132–139.
24. Smith ER, Hanssen E, McMahon LP, et al. Fetuin-A-containing calciprotein particles reduce mineral stress in the macrophage. *PLoS One*. 2013;8:e60904.
25. Aghagolzadeh P, Bachtler M, Bijarnia R, et al. Calcification of vascular smooth muscle cells is induced by secondary calciprotein particles and enhanced by tumor necrosis factor-α. *Atherosclerosis*. 2016;251:404–414.
26. Glatter O, Kratky O. *Small Angle X-Ray Scattering*. London, UK: Academic Press; 1982.